Dalton Transactions

PAPER

View Article Online
View Journal | View Issue

Check for updates

Cite this: *Dalton Trans.*, 2017, **46**, 5320

Anion exchange dynamics in the capture of perchlorate by a cationic Ag-based MOF†

Ian R. Colinas,[a] Kenneth K. Inglis,[b] Frédéric Blanc *[b] and Scott R. J. Oliver *[a]

We report a detailed study of the host–guest interaction for a cationic metal–organic framework that can reversibly capture perchlorate. The structural transformation and flexibility of silver 4,4′-bipyridine nitrate (SBN) upon formation of silver 4,4′-bipyridine perchlorate (SBP) was evaluated by monitoring the anion exchange dynamics using a combination of powder X-ray diffraction (PXRD) with multinuclear ^{13}C, ^{15}N and ^{109}Ag solid-state NMR spectra at different time intervals of the anion exchange. The structural transformation from SBN to SBP is complete within 70 minutes and was determined to take place by a solvent-mediated process. This pathway is confirmed by the morphological changes of the two crystalline materials observed by SEM. This key understanding may lead to application of this material towards perchlorate capture.

Received 7th February 2017,
Accepted 28th March 2017

DOI: 10.1039/c7dt00475c

rsc.li/dalton

Open Access Article. Published on 28 March 2017. Downloaded on 6/28/2026 4:55:07 AM.
This article is licensed under a Creative Commons Attribution 3.0 Unported Licence.

1. Introduction

Porous structures possessing weakly bound charge-balancing ions are essential for the development of new separation technologies and the removal of pollutant ions from aqueous environments. The capture of toxic perchlorate (ClO_4^-) presents unique challenges due its high solubility and non-complexing nature, making it highly mobile and resistant to traditional wastewater treatment technologies.[1] Perchlorate is an emerging trace contaminant in groundwater and has gained significant attention, as it has become widespread in many countries.[2] This anionic pollutant can block the uptake of iodide by the thyroid due to their equivalent charge and similar ionic radii. This blockage can disrupt the production of thyroid hormones and affect metabolism, possibly leading to hypothyroidism or mental retardation in fetuses and infants.[3] Perchlorate salts are used as the conventional solid oxidant in the industrial manufacture of rocket fuel, explosives, flares and fireworks.[4] Commercially available ion exchange resins are single use and exhibit limited thermal and chemical stability,[5] while other ion exchanging materials such as layered double hydroxides (LDHs) display poor selectivity[6] and adsorption capacity[7] for perchlorate. Higher performing ion exchangers are therefore sought to reversibly capture perchlorate at greater capacity and selectivity. In particular, metal–organic frameworks (MOFs) have gained significant attention in the selective capture of pollutants *via* ion exchange.[8]

Recently, MOFs have been under intense investigation due to their ability to exchange their intrapore or interlayer ions with other ionic species in solution. Their structural integrity is not compromised, which make these materials excellent candidates for the separation of pollutants.[9] The adsorptive separation of pollutant species in the gas phase, such as carbon dioxide or methane, is driven by the reversible dynamic behavior of the network, often referred to as "breathing". This action results in a change of interaction strength between the guest molecules and host framework due to framework displacement accompanied by a change in the unit cell volume.[10] There has been much less effort into understanding the structural flexibility and dynamic transformations that solid MOFs exhibit during adsorption and/or ion exchange. The mechanism by which such ion exchange processes take place has been proposed to be either by a solid state or a solvent-mediated transformation. In the case of a solid state transition, the ion exchange proceeds through the diffusion of free ions within the channels of the coordination polymer crystals. In contrast, the solvent-mediated process involves the dissolution of the initial coordination polymer followed by the formation and crystallization of a new coordination polymer from the solution phase.[11]

The structural transformations that coordination polymers undergo during ion exchange processes can be monitored by single crystal or powder X-ray diffraction (PXRD) of the MOF in combination with analytical measurements of the solution towards incoming and outgoing guests. If possible, single crystal X-ray crystallographic methods are preferred for the

[a]*University of California, Santa Cruz, Department of Chemistry and Biochemistry, 1156 High Street, Santa Cruz, California, 95064, USA. E-mail: soliver@ucsc.edu*
[b]*Department of Chemistry, Stephenson Institute for Renewable Energy, University of Liverpool, L69 7ZD, UK. E-mail: frederic.blanc@liverpool.ac.uk*

†Electronic supplementary information (ESI) available: Additional figures and NMR acquisition parameters. See DOI: 10.1039/c7dt00475c

This journal is © The Royal Society of Chemistry 2017

Open Access Article. Published on 28 March 2017. Downloaded on 6/28/2026 4:55:07 AM.
This article is licensed under a Creative Commons Attribution 3.0 Unported Licence.

exact structural determination of the new MOF phase upon adsorption. This methodology, however, provides limited structural information regarding the dynamic behavior of the framework during exchange due to the absence or sufficient size/quality of crystals. In contrast, magic-angle spinning (MAS) nuclear magnetic resonance (NMR) spectroscopy provides structural information about the local environment of various nuclei in solids, including both the metal nodes and the organic linkers of the MOFs.[12] Hence, NMR spectroscopy could be used in conjunction with XRD methods as a complementary technique for analyzing the exchange dynamics of MOF materials.[13] NMR is well suited to probe the structural flexibility and reversible dynamic behavior of a framework undergoing ion exchange. Jiang *et al.* reported the structural flexibility of a $Cu(bipy)_2(H_2O)_2(BF_4)$ (bipy = 4,4′-bipyridine) framework by chemisorption of probe molecules that could induce reversible structural changes. The transitions could be monitored by ^{11}B MAS NMR as a result of the change in polarization of the probe molecule and its interaction with the Cu(II) paramagnetic sites.[14]

In our previous work,[15] we reported the successful capture of aqueous perchlorate by Silver 4,4′-Bipyridine Nitrate (SBN)[16] to yield a Silver 4,4′-Bipyridine Perchlorate (SBP) MOF.[17] We showed that SBN effectively exchanged guest NO_3^- ions for ClO_4^- ions at a record capacity of 354 mg g^{-1} within 90 minutes. The material also selectively captured this pollutant in the presence of 50-fold molar SO_4^{2-} and CO_3^{2-}, suggesting this methodology could be applied to treat perchlorate pollution at underground plume sites. In addition, SBN displayed excellent reusability: 96% of SBP could be regenerated back to SBN over multiple cycles while maintaining uptake capacity. Anion exchange by metal bipyridine and pyrazine coordination polymers was evaluated by Schröder and coworkers utilizing several anions such as BF_4^- and PF_6^-.[18] The uptake was determined to be a solvent mediated process driven by the relative solubilities of the complex pairs as well as the relative hydration energy of the anions residing in the pores.

Herein, we report a study of the host–guest interaction of an Ag-bipy coordinated polymer during NO_3^- and ClO_4^- anion exchange dynamics. The structural transformation is followed by analysis of the $[Ag\text{-}bipy]^+$ material at different time intervals using PXRD to assess the presence of two structural phases corresponding to SBN and SBP. The structural transformation during exchange is further investigated by recording multinuclear ^{13}C, ^{15}N and ^{109}Ag cross-polarization (CP) MAS NMR spectra. ^{13}C [1.13% natural abundance (nat. ab.), nuclear spin $I = 1/2$] NMR is used to (semi)-quantify the SBN to SBP ratio during the anion exchange. ^{15}N (0.37% nat. ab., $I = 1/2$) NMR determines whether NO_3^- is present and probes the bonding between the nitrogen of bipy and silver *via* the scalar J coupling interaction and is further confirmed by ^{109}Ag (48.18% nat. ab., $I = 1/2$) NMR. In addition, this exchange is further investigated by inspecting the morphological changes of the crystalline materials by scanning electron microscopy (SEM).

2. Experimental

2.1 Synthesis

In short, a mixture of $AgNO_3$ ($AgNO_3$, Fisher, 99%, 0.1 g, 0.59 mmol), 4,4′-bipyridine (Acros Organics, 98%, 0.1 g, 0.64 mmol) and deionized water (10 mL) was stirred at room temperature for 3 days in a sealed beaker. Pale gray crystals were isolated after filtration and rinsed with water (10 mL) and acetone (5 mL) to yield SBN (0.187 g, 97.6% based on silver nitrate). Batch anion exchange experiments were carried out under ambient conditions by mildly stirring the ground SBN (80 mg, 0.25 mmol) with 50 mL deionized water and $NaClO_4$ (Fluka Analytical, 98%, 35 mg, 0.25 mmol). The post-exchange crystalline SBP product was recovered at the different time intervals by vacuum filtration and rinsed with water (10 mL) and acetone (5 mL).

2.2 Regeneration

The regeneration of SBN from SBP was carried out by stirring the ground SBP (80 mg, 0.22 mmol) in a 0.1 M $NaNO_3$ solution ($NaNO_3$, Fisher, 99%) at 70 °C for 24 h. The regeneration of the SBN was studied by recording the PXRD, ^{13}C, ^{15}N, ^{109}Ag CP MAS NMR data and SEM images after treatment of the SBP material with excess nitrate at 70 °C under stirring.

2.3 Characterization

PXRD data were measured on a Rigaku Americas Miniflex Plus diffractometer, scanning from 2 to 40° (2θ) at a rate of 2° min^{-1} with a 0.04° step size under Cu Kα radiation (λ = 1.5418 Å). Ion Chromatography (IC) analysis was performed to assess the perchlorate concentration using a Dionex ICS-3000 with an IonPac AS20 column and a detection limit of 3 μg L^{-1} (ppb). SEM data were collected with a FEI Quanta 3D Dualbeam microscope. Solid-state NMR experiments were performed at room temperature on a Wide Bore 400 MHz 9.4 T Bruker Avance III HD NMR spectrometer equipped with a 4 mm HXY triple-resonance MAS probe (in double resonance mode) for ^{13}C and ^{15}N and with a 4 mm HX MAS probe for ^{109}Ag or on a Wide Bore 850 MHz 20 T Bruker Avance II NMR spectrometer equipped with a 3.2 mm HXY triple-resonance MAS probe (in double resonance mode) for ^{13}C. Data acquisition was performed with cross polarization (CP) and SPINAL-64 heteronuclear decoupling.[19] Recycle delays ranging from 30 to 180 s were used and correspond to 1.3 × ^1H T_1 (measured by ^1H saturation recovery experiments). All other experimental details are given in Table S1.† The ^{13}C, ^{15}N and ^{109}Ag chemical shifts were referenced to the CH carbon of adamantane at 29.45 ppm,[20] glycine at 33.4 ppm (corresponding to liquid NH_3 at 0 ppm)[21] and a saturated solution of $AgNO_3$ in D_2O [with 0.24 M of $Fe(NO_3)_3$] at 0 ppm,[22] respectively. All samples were packed in air. Using the Haeberlen convention,[23] the principal components δ_{11}, δ_{22}, δ_{33} of the chemical shift tensors were defined such that $|\delta_{33} - \delta_{iso}| \geq |\delta_{11} - \delta_{iso}| \geq |\delta_{22} - \delta_{iso}|$ where δ_{iso} is the isotropic chemical shift and related to the principal components of the shielding tensor by $\delta_{iso} = (\delta_{11} + \delta_{22} + \delta_{33})/3$. The chemical shift anisotropy δ_{aniso} is defined as

Open Access Article. Published on 28 March 2017. Downloaded on 6/28/2026 4:55:07 AM.
This article is licensed under a Creative Commons Attribution 3.0 Unported Licence.

$\delta_{aniso} = \delta_{33} - \delta_{iso}$ and the deviation from axial symmetry given by the asymmetry parameter $\eta = (\delta_{22} - \delta_{11})/\delta_{aniso}$.

3. Results and discussion

The synthesis of SBN can be carried out at room temperature by the initial dissociation of silver nitrate followed by the self-assembly of the cationic polymer chains, charge balanced by nitrate ions. SBN can undergo quantitative anion exchange upon exposure to ClO_4^- in solution to yield SBP with a 99% conversion as determined by monitoring the concentration of ClO_4^- in solution from ion chromatography (IC). The PXRD data confirms the identity of the two crystalline phases as they match the theoretical patterns based on the single crystal solution (Fig. S1†).[16,17]

Both SBN and SBP structures consist of Ag(I) chelated by the nitrogens of two different (μ-2)-4,4′-bipyridine units that result in extended polymeric chains. The chains align parallel into a non π-stacked layer where the rings are coplanar with the plane of the page. The two structures differ in the arrangement of their subsequent layers. For SBN, the cationic layers are rotated by 90°, forming a criss-cross or T-shaped pattern in which half the pyridine rings π-stack in a staggered manner with a distance of 3.55 Å from the next layer (Fig. 1). In addition, half of the Ag(I) centers are dimerized and cross linked to the next layer by the formation of Ag–Ag bonds with a distance of 2.97(1) Å. In contrast, the cationic layers of SBP are eclipsed, resulting in π-stacking of all the pyridine rings and a shorter interlayer distance of 3.47 Å (Fig. 1). The Ag(I) centers have a long contact distance of 3.60(1) Å, which is well above the covalent range. These longer Ag–Ag distances allow for the spherical ClO_4^- anions to be more spread out between the polymeric interlayers. The ClO_4^- to Ag(I) distance is therefore greater for SBP than for SBN but closer contact of the anions to the bipyridine ***C***HC^{IV} in SBP (Table 1).

Table 1 Structural properties of SBN and SBP

	SBN	SBP
Distance		
Ag(I)–Ag(I)/Å	2.97(1)	3.60(1)
Anion O–Ag(I)/Å	2.826(17), 2.782(10)	2.945(15), 2.863(10)
Anion O–***C***HC^{IV}/Å	3.374(10)	3.352(10)
π-Stacking/Å	3.55	3.47
Angle		
N–Ag(I)–N/°	173.73	174.76

Based on the above structural considerations, it is clear that the two coordination polymers are structurally different in the arrangement of the cationic layers as well as the location of the anions. Such structural differences suggest that the anion exchange may proceed by a solvent-mediated process involving the initial dissolution of the SBN T-shaped polymers followed by the crystallization of eclipsed SBP polymers from the perchlorate solution (Fig. S2†).[15] In order to support this hypothesis, the anion exchange was monitored *versus* time by both PXRD (Fig. 2) and multinuclear MAS NMR (Fig. 3). After 10 minutes of exposure to ClO_4^-, the intensity of the low angle (002) peak decreases and a new set of peaks [*e.g.* 22° (2θ), corresponding to the (211) plane of the SBP crystalline phase] begin to appear, indicating initiation of the process.

After 25 minutes, the PXRD pattern is an approximately equal mixture of both the SBN and SBP crystal phases, indicating that the anions have been partially exchanged. The relative amounts of both phases were verified by measuring the residual concentration of perchlorate in the anion exchange solution at different time intervals with ion chromatography (Fig. S3†). The predominance of the SBP phase is observed after 40 minutes, where the low angle peaks corresponding to (001) and (100) of SBP are now higher intensity relative to the

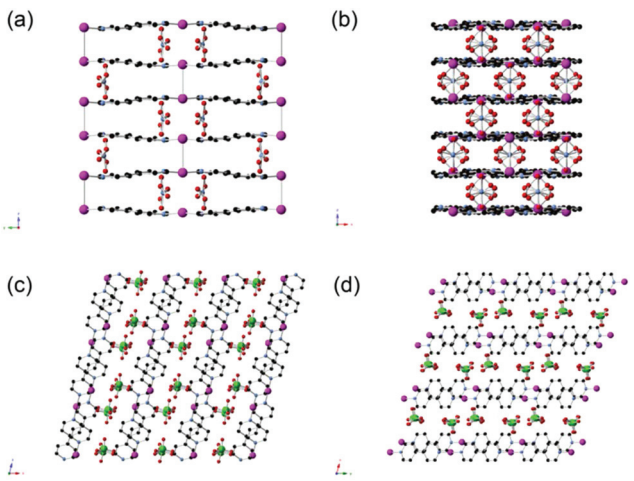

Fig. 1 (a) Crystallographic view of SBN in the "*a*" plane and (c) "*b*" plane. (b) Crystallographic view of SBP in the "*a*" plane and (d) "*c*" plane. The nitrate oxygens are disordered between two sites (Ag, magenta; N, blue; O, red; C, black; Cl, green).

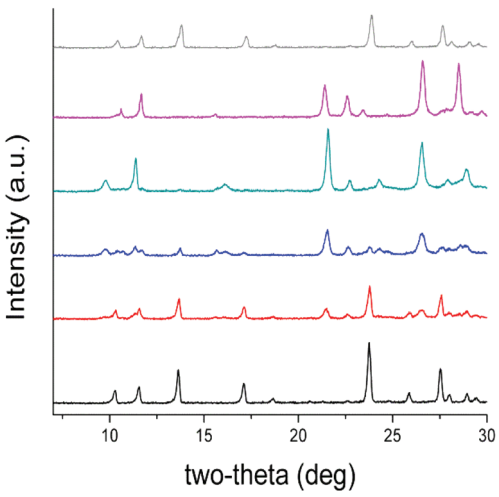

Fig. 2 PXRD patterns of the SBN/SBP anion exchange of SBN pre-exchange (black), after 10 min (red), 25 min (blue), 40 min (green), complete exchange to SBP after 70 min (purple), and regeneration to SBN (grey).

This journal is © The Royal Society of Chemistry 2017

Open Access Article. Published on 28 March 2017. Downloaded on 6/28/2026 4:55:07 AM.
This article is licensed under a Creative Commons Attribution 3.0 Unported Licence.

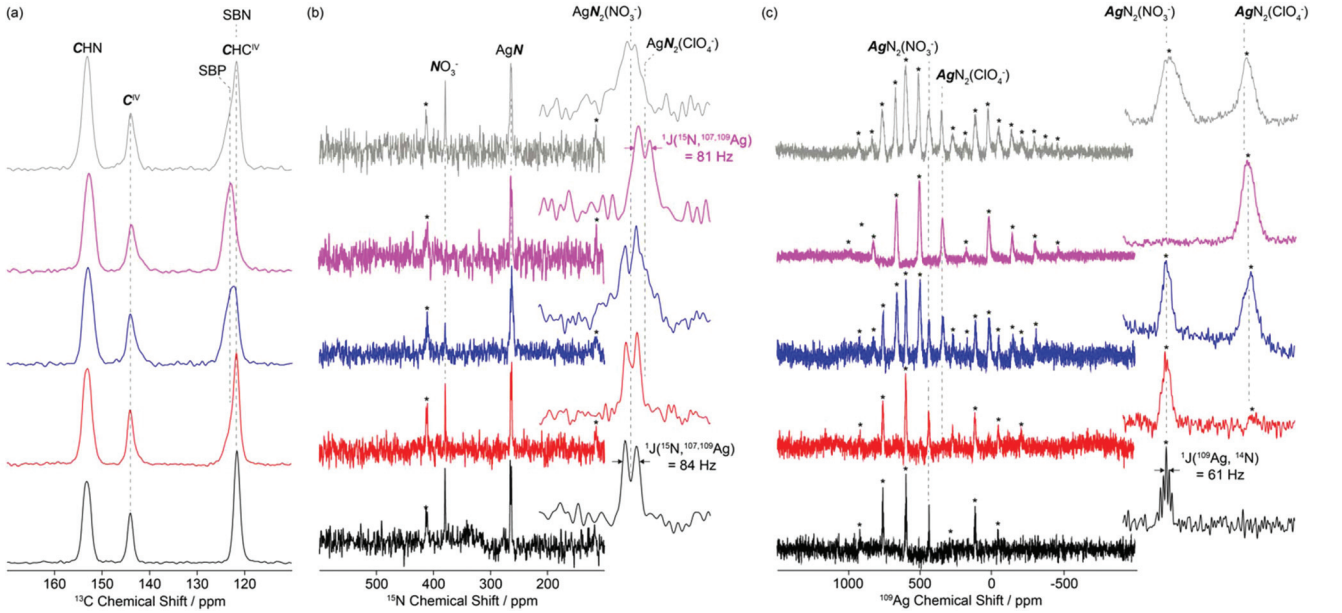

Fig. 3 (a) ^{13}C, (b) ^{15}N and (c) ^{109}Ag CP MAS NMR of the SBN/SBP anion exchange of SBN pre-exchange (black), after 10 min (red), 25 min (blue), complete exchange to SBP (purple) and regeneration back to SBN (grey). Spectral assignments are given in the figure. The ^{13}C spectra were obtained at 20 T while the ^{15}N and ^{109}Ag were obtained at 9.4 T. In (b), the insets show magnified views of the 280–250 ppm isotropic region of the AgN resonances. In (c), the insets show magnified views of the first left spinning sidebands in the 650–450 ppm region. Spinning sidebands are marked with asterisks (*).

peaks of SBN. After 70 minutes, the anion exchange is complete and the PXRD pattern is pure phase SBP (see below for recovery to SBN). In addition, a shift in the (001) and (100) phases to a higher 2-theta indicates that the *d*-spacing decreased, likely due to a contraction of the structure upon completion of the anion exchange.

The ^{13}C CP MAS NMR spectra of SBN and SBP (black and purple spectra, Fig. 3a) obtained at 20 T show three different isotropic resonances δ_{iso} at 153.3–152.7, 144.1–143.8 and 123.3–121.7 ppm for the individual carbons in the asymmetric unit and correspond to the ***C***HN, C^{IV} and ***C***HC^{IV} environments in the 4,4′-bipyridine ligand, respectively. As the NO_3^-–ClO_4^- anion exchange progressed by dissolution of SBN and subsequent capture of the ClO_4^- by the crystallization of SBP, a downfield shift of around 1.6 ppm is clearly observed in the signal of the ***C***HC^{IV} carbon (Fig. 3a, S4 and S5†).

Comparison of the ***C***HC^{IV} signal intensities at 121.7 and 123.3 ppm for SBN and SBP, respectively, enables a semi-quantitative analysis of the rates of exchanges to be monitored (note that while CP MAS NMR experiments are not quantitative, integration is performed on the same ***C***HC^{IV} carbon, therefore a SBN/SBP ratio could be approximately estimated). After 10 and 25 minutes, approximately 20 and 60% of SBN have been transformed into SBP, respectively. Partial degree of exchange at these time intervals agrees well with the PXRD data (red and blue patterns, Fig. 3).

This shift difference between the ***C***HC^{IV} carbon in SBN and SBP is probably due to the higher degree of carbon deshielding caused by the perchlorate anions. As stated above, the cationic layers of SBP have a shorter π-stacking distance relative to SBN due to the fully eclipsed arrangement of the Ag-bipy chains. This shorter distance causes the ClO_4^- anions to be more tightly packed between the aromatic rings and in turn a longer Ag–O distance. Consequently, the ClO_4^- oxygens are in closer proximity to ***C***HC^{IV} carbon, resulting in a higher degree of deshielding as reflected by the observed chemical shift.

The ^{15}N CP MAS NMR spectrum of SBN (Fig. 3b, black) at 9.4 T reveals two isotropic resonances δ_{iso} at 379.3 and 263.9 ppm and are assigned to the NO_3^- anions and the nitrogen of the bipy ligand, respectively. A doublet of 84 Hz is observed for the former resonance and results from the indirect scalar $^1J(^{15}N, ^{107,109}Ag)$ coupling arising from coordination of the nitrogen atoms of bipy to the silver atoms, as expected from the crystal structure (Fig. 1). Similar scalar coupling constants were obtained in a series of linear or almost linear two-coordinate $[Ag(NH_3)_2]^+$ ions.[24]

The ^{109}Ag CP MAS NMR[25] spectrum of SBN (purple, Fig. 3c) shows a series of intense spinning sidebands spanning over approximately 1000 ppm, in agreement with a large chemical shift anisotropy of $\delta_{aniso} = -774$ ppm. Note that the relatively low signal to noise ratio of this ^{109}Ag spectrum arises from the very low magnetic moments of this nucleus. A single isotropic resonance appears at $\delta_{iso} = 438.5$ ppm and is consistent with a single silver atom environment in SBN. This resonance is a quintet with a spacing of 61 Hz, corresponding to the indirect scalar coupling between ^{109}Ag and ^{14}N (99.63% nat. ab., $I = 1$). The approximate 1 : 2 : 3 : 2 : 1 relative intensity of the quintet is expected for coupling to two equivalent $I = 1$ nuclei and the crystal structure of SBN presenting a silver atom nitrogen-bonded by two bipy ligands. Note that the

Open Access Article. Published on 28 March 2017. Downloaded on 6/28/2026 4:55:07 AM.
This article is licensed under a Creative Commons Attribution 3.0 Unported Licence.

$^1J(^{15}N, ^{107,109}Ag) : ^1J(^{109}Ag, ^{14}N)$ ratio is 1.38, close to the expected $^{15}N : ^{14}N$ magnetic moment ratio of 1.40. Additionally, the spinning sideband manifold yields an axially symmetric chemical shift tensor (*i.e.* $\eta = 0$). This observation agrees well with the almost linear environment[23] of the N–Ag(I)–N moieties in the bipy–Ag–bipy polymers (173.73°, Table 1).

As SBN is converted into SBP by addition of ClO_4^-, the relative ratio of the NO_3^- anions and the bipy ligand signals at 379.3 and 263.9 ppm in the ^{15}N CP MAS NMR spectra decreases, until a single nitrogen environment is detected upon total exchange to SBP. The corresponding ^{15}N spectrum (purple, Fig. 3b) shows a doublet with $^1J(^{15}N, ^{107,109}Ag)$ = 81 Hz centred at δ_{iso} = 261.4 ppm. This signal is due to the nitrogen atoms of bipy that are bonded to Ag. No resonance could be detected at 379.3 ppm in SBP, consistent with the complete NO_3^-–ClO_4^- anion exchange as seen by PXRD. The very small difference in chemical shift between the nitrogen atoms of bipy in SBN (263.9 ppm) and SBP (261.4 ppm) likely arises from the greater deshielding of the bipy nitrogen in SBN by the NO_3^- that is in closer proximity to the silver atom. The ^{15}N CP MAS NMR spectra for SBN and SBP are therefore consistent with the ^{13}C CP MAS NMR spectra in the arrangement of the Ag-bipy cationic layers upon exchange of NO_3^- for ClO_4^- perchlorate anions.

Upon SBN/SBP anion exchange, the ^{109}Ag CP MAS NMR spectra (Fig. 3c) reveal the appearance of an additional isotropic resonance at approximately δ_{iso} = 341 ppm. Its intensity increases with ClO_4^- content and is attributed to the $[Ag\text{-}bipy]^+$ moiety in SBP. Upon total exchange, the ^{109}Ag signal of SBN completely disappears, in agreement with the PXRD, ^{13}C and ^{15}N data discussed above. Note that no $^1J(^{109}Ag, ^{14}N)$ scalar coupling could be clearly detected in the ^{109}Ag CP MAS NMR spectrum of SBP, probably resulting from slightly broader NMR lines and disorder. An axially symmetric ^{109}Ag chemical shift tensor with δ_{aniso} = −776 ppm and $\eta = 0$ is also obtained, the later value in agreement with the linear N–Ag(I)–N angle in SBP (Table 1).

The change in morphology of the SBN crystals during anion exchange with ClO_4^- was investigated by performing batch tests experiments, stopping the reaction at various time intervals to analyze the resulting crystals by SEM (Fig. 4). Initially, the synthesis of SBN yields smooth block-shaped crystals with an average width of 4 to 10 μm (black, top left, Fig. 4). Upon 10 min of exposure of the SBN crystals to the ClO_4^- aqueous solution, the smooth block shaped crystals began to display indentations at the surface (red, Fig. 4). These indentations show that the new SBP phase is beginning to take form on the SBN crystals, similar to that reported by Schröder and coworkers for $[Ag(4,4\text{-bipy})^+][BF_4^-]$ to $[Ag(4,4\text{-bipy})^+][NO_3^-]$.[18] After 25 min, small needles corresponding to the SBP crystal phase are observed in addition to SBN blocks with indentations (blue, Fig. 4). After 40 min, the crystals have lost their block-shaped morphology and consist primarily of bundles of needles that appear to be nucleated from the SBN block crystals (green, Fig. 4). The anion exchange is complete after 70 minutes and only long SBP needles could be identified (purple, Fig. 4), with average length 12 to 15 μm and width 2 to 4 μm.

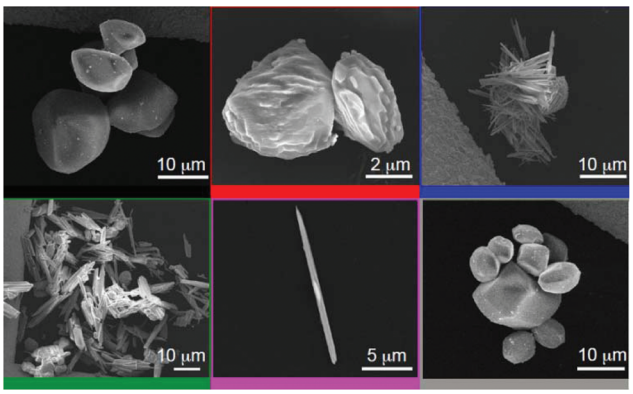

Fig. 4 SEM images of SBN pre-exchange (black, top left) and the solid after 10 min (red), 25 min (blue), 40 min (green), complete exchange to SBP (purple), and the first regeneration to SBN (grey).

The gradual change in morphology of the SBN block crystals to SBP needles upon exposure to ClO_4^- solution confirms that the structural transformation between the two coordination polymers occurs by a solvent-mediated process, consistent with the PXRD patterns and MAS NMR spectra described above. The self propagating growth of a new crystal phase from a parent phase has been proposed to facilitate the exchange of anions in the inside core of $[Ag(4,4\text{-bipy})^+][BF_4^-]$ crystals undergoing the structural transformation to $[Ag(4,4\text{-bipy})^+][NO_3]$.[11]

The reversibility of the anion exchange was demonstrated in our previous work and seven cycles of perchlorate uptake were monitored by PXRD.[15] The metastability of the $[Ag\text{-}bipy]^+$ solids allow for the reversible solvent mediated transformation that can be controlled by the concentration of the incoming anions and temperature. The lower solubility of SBP as well as its higher stability due to the greater degree of π-stacking account for the rapid SBN to SBP transition. In contrast, the re-intercalation of nitrate is a less favoured process due to the larger hydration energy of nitrate. Additionally, SBN has a lower stability due to the partial π-stacking.

The regeneration of the SBN was further studied by recording the PXRD, ^{13}C, ^{15}N, ^{109}Ag CP MAS NMR data and SEM images after treatment of the SBP material with excess nitrate at 70 °C under stirring (grey spectra, Fig. 3 and 4). The heat promotes the dissolution of the SBP polymers, while the excess nitrate shifts the dynamic equilibrium of the exchange to return to block shaped crystals with morphology identical to the as-synthesized SBN material (*cf.* black and grey SEMs, Fig. 4). The corresponding PXRD, ^{13}C and ^{109}Ag NMR data showed that although SBN has been mostly regenerated, approximately 10% of SBP is still present (as evidenced by integration of the NMR spectra and PXRD peaks).

4. Conclusion

This work shows by multiple complementary solid state methods that ClO_4^- uptake by Silver 4,4′-Bipyridine Nitrate (SBN) $[Ag\text{-}bipy^+][NO_3^-]$ occurs *via* a solvent-mediated process

 This journal is © The Royal Society of Chemistry 2017

Open Access Article. Published on 28 March 2017. Downloaded on 6/28/2026 4:55:07 AM.
This article is licensed under a Creative Commons Attribution 3.0 Unported Licence.

to yield Silver 4,4′-Bipyridine Perchlorate (SBP). The structural features of the silver coordination polymers in terms of π-stacking and electrostatics concur with the dynamics of the anion exchange process. All three characterization methods show that the two crystalline phases are present throughout the anion exchange process. This study provides evidence of the structural flexibility displayed by the interaction of cationic [Ag-bipy^{+}] MOFs with different adsorbates upon anion exchange. Such understanding of structural dynamics is crucial for the rational design of these and related MOFs toward the selective capture of environmental pollutant oxo-anions such as perchlorate, chromate and arsenate. Reusability over many cycles is also crucial for the cost-effective deployment of these materials. The formation of new crystals on each exchange cycle circumvents the degradation issues of current ion exchange solids such as resins and LDHs that force them to be single-use.

Acknowledgements

This work was supported by the National Science Foundation under Grant No. 1603754 from the CBET Environmental Engineering Program. I. R. C. was supported by a fellowship from the IMSD program funded by the National Institute of Health under Grant No. 2R25GM058903-17 and thanks Nick J. Brownbill (University of Liverpool, Department of Chemistry) for technical assistance with the NMR spectrometer. The PXRD data in this work were recorded on an instrument supported by the NSF Major Research Instrumentation (MRI) Program under Grant No. 1126845. K. K. I. thanks the EPSRC for a studentship. The UK 850 MHz solid-state NMR Facility used in this research was funded by EPSRC and BBSRC (contract reference PR140003), as well as the University of Warwick including *via* part funding through Birmingham Science City Advanced Materials Projects 1 and 2 supported by Advantage West Midlands (AWM) and the European Regional Development Fund (ERDF). Collaborative assistance from the 850 MHz Facility Manager (Dr Dinu Iuga, University of Warwick) is acknowledged. We also acknowledge Dr Tom Yuzvinsky and the W. M. Keck Center for Nanoscale Optofluidics at UC Santa Cruz for the use and assistance in image acquisition on the FEI Quanta 3D Dualbeam microscope. Original data are available at the University of Liverpool's DataCat repository at http://datacat.liverpool.ac.uk/id/eprint/283.

References

1 E. T. Urbansky and M. R. Schock, *J. Environ. Manage.*, 1999, **56**, 79–95.
2 Y. Yang, N. Gao, W. Chu, Y. Zhang and Y. Ma, *J. Hazard. Mater.*, 2012, **209–210**, 318–325.
3 A. Srinivasan and T. Viraraghavan, *Int. J. Environ. Res. Public Health*, 2009, **6**, 1418–1442.
4 P. K. Dasgupta, P. K. Martinelango, W. A. Jackson, T. A. Anderson, K. Tian, R. W. Tock and S. Rajagopalan, *Environ. Sci. Technol.*, 2005, **39**, 1569–1575.
5 W. Song, X. Xu, X. Tan, Y. Wang, J. Ling, B. Gao and Q. Yue, *Carbohydr. Polym.*, 2015, **115**, 432–438.
6 K.-H. Goh, T.-T. Lim and Z. Dong, *Water Res.*, 2008, **42**, 1343–1368.
7 J. Y. Kim, S. Komarneni, R. Parette, F. Cannon and H. Katsuki, *Appl. Clay Sci.*, 2011, **51**, 158–164.
8 S. R. J. Oliver, *Chem. Soc. Rev.*, 2009, **38**, 1868.
9 R. Custelcean, T. J. Haverlock and B. A. Moyer, *Inorg. Chem.*, 2006, **45**, 6446–6452.
10 A. Schneemann, V. Bon, I. Schwedler, I. Senkovska, S. Kaskel and R. A. Fischer, *Chem. Soc. Rev.*, 2014, **43**, 6062–6096.
11 C. Thompson, N. R. Champness, A. N. Khlobystov, C. J. Roberts, M. Schroder, S. J. B. Tendler and M. J. Wilkinson, *J. Microsc.*, 2004, **214**, 261–271.
12 D. D. Laws, H.-M. L. Bitter and A. Jerschow, *Angew. Chem., Int. Ed.*, 2002, **41**, 3096–3129.
13 H. Hoffmann, M. Debowski, P. Müller, S. Paasch, I. Senkovska, S. Kaskel and E. Brunner, *Materials*, 2012, **5**, 2537–2572.
14 Y. Jiang, J. Huang, B. Kasumaj, G. Jeschke, M. Hunger, T. Mallat and A. Baiker, *J. Am. Chem. Soc.*, 2009, **131**, 2058–2059.
15 I. R. Colinas, R. C. Silva and S. R. J. Oliver, *Environ. Sci. Technol.*, 2016, **50**, 1949–1954.
16 O. M. Yaghi and L. Hailian, *J. Am. Chem. Soc.*, 1996, **118**, 295–296.
17 L.-S. Wang, J.-F. Zhang and S.-P. Yang, *Acta Crystallogr., Sect. E: Struct. Rep. Online*, 2004, **60**, m1484–m1486.
18 X. Cui, A. N. Khlobystov, X. Chen, D. H. Marsh, A. J. Blake, W. Lewis, N. R. Champness, C. J. Roberts and M. Schröder, *Chem. – Eur. J.*, 2009, **15**, 8861–8873.
19 B. M. Fung, A. K. Khitrin and K. Ermolaev, *J. Magn. Reson.*, 2000, **142**, 97–101.
20 C. R. Morcombe and K. W. Zilm, *J. Magn. Reson.*, 2003, **162**, 479–486.
21 P. Bertani, J. Raya and B. Bechinger, *Solid State Nucl. Magn. Reson.*, 2014, **61–62**, 15–18.
22 J. K. Plischke, A. J. Benesi and M. A. Vannice, *J. Phys. Chem.*, 1992, **96**, 3799–3806.
23 M. Mehring, *Principles of High Resolution NMR in Solids*, Springer Verlag, Berlin, 2nd edn, 1983.
24 G. A. Bowmaker, R. K. Harris, B. Assadollahzadeh, D. C. Apperley, P. Hodgkinson and P. Amornsakchai, *Magn. Reson. Chem.*, 2004, **42**, 819–826.
25 L. H. Merwin and A. Sebald, *J. Magn. Reson.*, 1992, **97**, 628–631.